

## RESEARCH ARTICLE

### *Philosophical Magazine* – Topological Quantum Glassiness

Claudio Castelnovo<sup>a\*</sup> and Claudio Chamon<sup>b</sup>

<sup>a</sup> *SEPnet and Hubbard Theory Consortium, Department of Physics, Royal Holloway University of London, Egham TW20 0EX, UK*

<sup>b</sup> *Department of Physics, Boston University, Boston MA, 02215 USA*

(v1.0 released July 2011)

Quantum tunneling often allows pathways to relaxation past energy barriers which are otherwise hard to overcome classically at low temperatures. However, this is not always the case. In this paper we provide exactly solvable examples where the barriers each system encounters on its approach to lower and lower energy states become increasingly wide and eventually scale with the system size. If the environment couples *locally* to the physical degrees of freedom in the system, tunnelling under these barriers requires processes whose order in perturbation theory is proportional to the width of the barrier. This results in quantum relaxation rates that are exponentially suppressed in system size: For these quantum systems, no *physical* bath can provide a mechanism for relaxation that is not dynamically arrested at low temperatures. The examples discussed here are drawn from three dimensional generalizations of Kitaev's toric code, originally devised in the context of topological quantum computing. They are devoid of any local order parameters or symmetry breaking and are examples of topological quantum glasses. We construct systems that have slow dynamics similar to either strong or fragile glasses. The example with fragile-like relaxation is interesting in that the topological defects are neither open strings or regular open membranes, but fractal objects with dimension  $d^* = \ln 3 / \ln 2$ .

**Keywords:** glassiness; stochastic processes; quantum tunneling

#### 1. Introduction: How slow is slow?

The problem of the approach to equilibrium is a formidable one. Nature provides us with plenty of examples of systems that simply do not equilibrate in any experimentally accessible times, starting from a material that is so commonly accessible to become synonym of an entire field of research:  $\text{SiO}_2$ , *glass* [1]. A great deal of effort has been directed, both by physicists and chemists alike, to the question of how we can understand and describe these systems when they encounter dynamical obstructions in their attempted path to thermal equilibration. In spite of much research, however, a complete theoretical description of the glass transition remains an open problem.

Understanding the origin of long equilibration time scales is both of fundamental significance from a theoretical point of view and of great importance from a technological point of view. Uncovering the reasons why systems fall out of equilibrium might enable us to manipulate them, either hindering or enhancing the slow dynamics depending on the specific application. Advancements on understanding the properties of glassy materials would have implications to problems ranging from biology to petroleum recovery.

---

\*Corresponding author. Email: Claudio.Castelnovo@rhul.ac.uk

Before we begin our discussion, one should decide on a working definition of slow dynamics: *how slow is slow?* On the one hand, one can set a threshold – for instance, the famed viscosity of  $10^{13}$  Poise [1] – beyond which a system is said to be in a glassy state. A classification can then be developed based on how quickly the time scales grow as a function of some natural tuning parameter that leads the system into such state (e.g., temperature or concentration). According to this classification, if the parameter is temperature, one distinguishes between strong and fragile glasses if the equilibration time scales grow in an Arrhenius form  $\tau \sim \exp[\Delta/T]$  or faster, respectively. Examples of the latter are the exponential inverse temperature square behavior,  $\tau \sim \exp[\Delta^2/T^2]$ , and the Vogel-Fulcher law for a true glass transition at finite  $T_0$ ,  $\tau \sim \exp[\Delta/(T - T_0)]$ .

On the other hand, one can classify systems *in their glassy state* by looking at how fast their large time scales grow with system size. While in a finite system all time scales are strictly speaking finite,<sup>1</sup> they can exhibit a dependence on system size. In general, one can account for three different scenarios. (i) There could be no size dependence at all. For instance, a purely Arrhenius behaviour with a local energy barrier  $\Delta$  can lead to time scales  $\sim \exp(\Delta/T)$  that are independent of the size of the system. (ii) Time scales can grow polynomially in system size,  $\tau \sim \text{poly}(L)$ . For example, this is the case of critical slowing down and diffusive modes. Finally, (iii) time scales can grow exponentially in system size,  $\tau \sim \exp(L)$ .<sup>2</sup> [In the following we shall use the short hand notation  $\tau \sim \exp(L)$  to denote generic exponential time scales of the form  $\exp(aL^b)$ .] Examples include the Sherrington-Kirkpatrick model [2] and  $p$ -spin glasses [3, 4].

Drawing a line between time scales that grow polynomially vs. exponentially in system size can be understood within the framework of computational complexity: Nature itself is a computer (which could in turn be simulated in a universal digital computer), running its algorithm for dynamical evolution. Any system thermalizes if the algorithm is allowed to run indefinitely. However, in finite times one has to come to terms with how efficient the dynamical evolution algorithm is. The system size  $L$  is the size of the problem and systems whose equilibration times grow exponentially in  $L$  correspond to computationally hard problems for nature's algorithm.

In this article we focus on the system size dependence of equilibration time scales, in particular in quantum systems. In Sec. 2, we argue that any classical system whose relaxation is exponential in  $L$ , when endowed with local quantum dynamics, enters a quantum glass state (exponential in system size). The converse is not true. Quantum glasses exist that ‘melt’ at any finite temperature, with the appearance of time scales that are polynomial in system size. In Sec. 3 we provide three examples of this behaviour.

We note that exponentially long times naturally arise in systems undergoing spontaneous symmetry breaking. For example, going from positive to negative magnetization in the ordered phase of an Ising ferromagnet takes an exponentially large time in system size. These states however are distinguished by local order parameters (e.g., the local magnetization), which allow one to make significant progress in understanding their dynamics in terms of nucleation, domain growth and coarsening. In this paper we focus instead on systems where exponential relaxation time scales appear in the absence of local order parameters and symmetry breaking. At the quantum mechanical level, a natural context where to look for ground states

<sup>1</sup>Note however that these time scales may already be in practice longer than any experimentally accessible times.

<sup>2</sup>In any realistic (i.e., extensive) system, time scales cannot grow faster than exponential in the volume of the system.

without local order and without explicit disorder in the Hamiltonian or bath parameters is that of topologically ordered systems [5, 6]. Indeed the examples of quantum glasses we put forward in Sec. 3 are inspired by toy lattice models for topological order [7] and ought perhaps to be called *topological quantum glasses*. A brief account on the physics of this family of quantum glasses, and in particular of the example in Sec. 3.2, was discussed by one of the authors in Ref. [8].

Finally, in Sec. 4 we briefly comment on general approaches to characterise dynamical quantum systems and how – due to the characteristic exponential dependence on system size – one should beware of truncating perturbative approaches when studying quantum glasses, as they lead to reducible dynamics within disconnected sectors.

## 2. Classical and quantum glasses

It is often the case that quantum tunneling allows relaxation past energy barriers which are otherwise hard to overcome classically at low temperatures. For instance, the growth of equilibration time scales due to Arrhenius activated behaviour from a local, finite barrier  $\tau \sim \exp(\Delta/T)$  is eventually cut off at sufficiently low temperatures by temperature-independent tunneling across the barrier,  $\tau_q \sim \Delta/t$  where  $t$  is some quantum mechanical amplitude for the process.<sup>1</sup>

In general, classical systems that enter a glass state exhibit equilibration time scales that grow exponentially in system size.<sup>2</sup> The origin of such characteristic exponential dependence lies in the appearance of large energy barriers between the glassy free energy minima, whose height and width grow with the system size.

What happens if we take a classical system with  $\tau \sim \exp(L)$  and lower the temperature to zero, where coherent quantum mechanical processes become active? As we shall argue hereafter, the fact that the barriers grow with system size has a dramatic effect on the quantum mechanical relaxation time scales. Realistically, we assume that only local terms are allowed in the tunneling Hamiltonian – for instance, a transverse field of magnitude  $t$  that flips individual spins in a localised spin system. Wide barriers mean that the system has to visit a large number  $N_s \sim \text{poly}(L)$  of excited states in its journey from one side to the other of the barrier. Quantum mechanically this process is strongly suppressed:  $\tau_q \sim (U/t)^{N_s}$ , where  $U$  is the energy scale of the intermediate virtual states. Consequently, the quantum mechanical relaxation time scale acquires also a system size dependence of *exponential form*,  $\tau_q \sim \exp[N_s \ln(U/t)] \sim \exp(L)$ .

We conclude that a classical model with  $\tau \sim \exp(L)$  remains exponentially slow at  $T = 0$  even if (local) quantum tunneling processes are allowed. A whole family of quantum glasses can thus be derived directly from classical glassy systems by replacing temperature with local quantum dynamics. One might wonder whether the converse is true: Are there quantum glasses that do not have a classical parent? In other words, are there quantum systems that have exponential relaxation times  $\tau_q \sim \exp(L)$  at  $T = 0$ , but that immediately ‘melt’ to  $\tau \lesssim \text{poly}(L)$  as soon as  $T > 0$ ? In Sec. 3 we will answer positively to this question by explicit construction of local Hamiltonians that are examples of *purely quantum* glasses.

<sup>1</sup>These time scales are dimensionless for convenience. They are intended as factors multiplying the characteristic microscopic time of the system in the absence of barriers. For instance, in the quantum mechanical tunnelling case, the characteristic time would be dictated by the inverse hopping amplitude,  $1/t$ .

<sup>2</sup>Systems where the glass transition occurs in the zero temperature limit ought to be treated with care, as the order of limits (thermodynamic vs.  $T \rightarrow 0$ ) matters. For instance, time scales that are exponential in system size with a trivial Arrhenius activated prefactor  $\exp(\Delta/T)$  diverge in the  $T \rightarrow 0$  limit irrespective of system size.

### 3. Examples of quantum glasses without disorder

In order to construct our quantum Hamiltonians, we shall draw inspiration from two rather distinct areas: (i) classical kinetically constrained models, where slow dynamics appear without disorder; and (ii) spin models for topological order, which exhibit gapped quantum ground states devoid of any local order parameters or symmetry breaking.

Kinetically constrained models allowed to make progress on the study of the classical glass transition by investigating systems in which the equilibrium properties are easy to understand, but the dynamics are non-trivial due to kinetic constraints (for a review, see Ref. [9]). Simple lattice models are constructed embodying the notion that there are jammed and unjammed regions in glass formers described by a discrete state, which is representable in terms of Ising spin variables [10]. One particularly interesting class is that of spin plaquette models with nontrivial classical energy function and unconstrained spin dynamics, which can be equivalently described in terms of non-interacting defect variables with rather constrained multi-defect dynamics [11–14]. The thermodynamics of these systems is therefore trivial, while their dynamics is not, displaying a rich non-equilibrium behaviour (ageing, for instance).

Topological order is a relatively recent concept in systems of strongly interacting particles [5, 6]. Some quantum phases of matter, in contrast to common examples like crystals and magnets, are not characterized by a local order parameter and broken symmetries. Instead, they are characterized by a ground state degeneracy (when the system is defined on a torus or other surface of higher genus) that cannot be lifted by any local perturbation. This degeneracy is topological in nature and it is intimately related to quantum number fractionalization. The robustness of the topological degeneracy against local noise due to the environment is at the core of topological quantum computation [7].

Strong correlations that lead to these exotic quantum spectral properties can also impose kinetic constraints similar to those studied in the context of glass formers. Here we presents concrete examples of systems that have local Hamiltonians with no quenched disorder, exactly solvable spectra and topologically ordered quantum ground states. In these examples, not only do the classical thermal barriers grow with decreasing temperature, but also the widths of the quantum tunneling barriers do, in such a way that quantum processes are even more severely suppressed than classical ones at low temperatures. The origin of this behavior is the fact that *any* bath couples *locally* to the physical degrees of freedom of the system and it can only flip large objects through virtual processes of large order in the system-bath coupling. For these quantum systems, no *physical* bath can provide a mechanism for relaxation that is *not* dynamically arrested at low temperatures.

We first discuss a two-dimensional (2D) quantum system with strong glass-like relaxation times when in contact with a restricted class of thermal baths; this example is used to clarify the issue of how a given Hamiltonian requires a minimum number of degrees of freedom that the bath must locally control for the system to be able to equilibrate. The second example is a three-dimensional quantum system with strong glass-like relaxation times for any class of baths that couple locally to physical degrees of freedom of the system. The third example is a three-dimensional quantum system with fragile glass-like relaxation times.

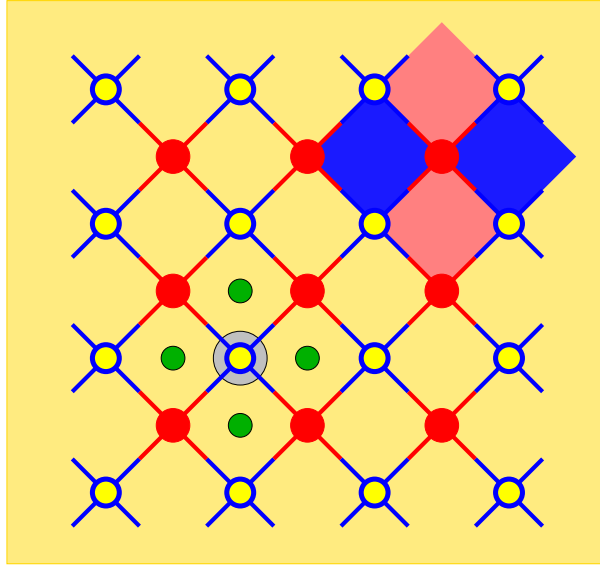


Figure 1. Square lattice, with spin operators defined on the sites. The square lattice is bipartite, and the two sets of points  $A, B$  are shown in red solid dots and blue open circles. A diamond contains 4 vertices in an elementary plaquette, and the diamonds can also be divided into two sets (forming a red/blue checkerboard) according to which sublattice their topmost vertices belong to. Four-spin operators are defined on each plaquette using the  $\sigma^x$  and  $\sigma^y$  components of the spin, as described in the text. The green dots correspond to “defects” that are generated by applying a  $\sigma^z$  to the site encircled.

### 3.1. Warmup: 2D example

The first model is constructed on a two-dimensional (2D) square lattice, shown in Fig. 1. Each site can be labeled by  $i, j \in \mathbb{Z}$  that index a site in the Bravais lattice spanned by the primitive vectors  $\mathbf{a}_1 = (1, 1)/\sqrt{2}$  and  $\mathbf{a}_2 = (-1, 1)/\sqrt{2}$ . To shorten the notation, define a superindex  $I \equiv (i, j)$ . At every lattice site  $I$  one defines quantum spin  $S = 1/2$  operators  $\sigma_I^x$ ,  $\sigma_I^y$ , and  $\sigma_I^z$ . The square lattice is bipartite: it contains two sets of sites, which we label  $A$  and  $B$ , and which are shown in red and blue color in Fig. 1.

Let us define the quantum Hamiltonian in terms of the spins  $\sigma_I$ . Here we follow an approach similar to that of Kitaev, who constructed in a beautiful paper model quantum Hamiltonians that are exactly solvable [7]. In those models, the spins resided on links in planar lattices, but it is possible to carry out similar constructions with spins defined on vertices [15], as it is done here. Later on we show how the construction with spins on vertices can be generalized to 3D lattices.

Define a *diamond* cell  $P_I$  as the set of four lattice sites in an elementary plaquette with site  $I$  at its top. The four vertices are indexed by  $J_n(I)$ , for  $n = 1, \dots, 4$ , with one of the vertices  $J_1(I) = I$ . The four labels are assigned in such a way that the pairs  $\{J_1, J_3\}, \{J_2, J_4\}$  are diagonally opposite sites from one another. Explicitly,  $J_1(I) = I \equiv (i, j)$ ,  $J_2(I) \equiv (i - 1, j)$ ,  $J_3(I) \equiv (i - 1, j - 1)$ , and  $J_4(I) \equiv (i, j - 1)$ . It is simple to see that the total number of diamonds equals the number of spins: each lattice site  $I$  is the top vertex of a single diamond. The one-to-one relation between a site  $I$  and the diamond  $P_I$  allows us to partition diamonds into two sets  $A$  and  $B$  (and color the corresponding diamonds red and blue, as shown in Fig. 1).

Now define the operators  $\mathcal{O}_I$  as

$$\mathcal{O}_I = \sigma_{J_1(I)}^y \sigma_{J_2(I)}^x \sigma_{J_3(I)}^y \sigma_{J_4(I)}^x. \quad (1)$$

These operators commute,  $[\mathcal{O}_I, \mathcal{O}_{I'}] = 0$  for all pairs  $I, I'$ . It is simple to see how: two diamonds  $P_I$  and  $P_{I'}$  can share 0, 1, or, 2 spins ( $I \neq I'$ ). If they share 0 spins,

they trivially commute. If they share 1 spin, the component (x,y or z) of  $\sigma$  for that shared spin coincides for both  $\mathcal{O}_I$  and  $\mathcal{O}_{I'}$  (the two diamonds touch along one of their diagonals). If they share 2 spins, the components of  $\sigma$  used in the definition of  $\mathcal{O}_I$  and  $\mathcal{O}_{I'}$  are different for both spins, there is a minus sign from commuting the x and y components of the spin operators from each of the shared spins, and the two minus signs cancel each other.

Consider the system Hamiltonian

$$\hat{H} = -h \sum_I \mathcal{O}_I, \quad (2)$$

which is trivially written in terms of the  $\mathcal{O}_I$  operators, but complicated in terms of the original spins  $\sigma_I$ . Because the  $\mathcal{O}_I$  commute, the eigenvalues of the Hamiltonian can be labeled by the list of eigenvalues  $\{O_I\}$  of all the  $\mathcal{O}_I$ . Note that  $\mathcal{O}_I^2 = \mathbb{I}$ , and each  $O_I = \pm 1$ . In particular, the ground state corresponds to  $O_I = 1$  for all  $I$ .

Because the number of spins equals the number  $N$  of sites, one may naively expect that the list  $\{O_I = \pm 1\}$  exhausts the  $2^N$  states in the Hilbert space, spanned by  $\{\sigma_I^z = \pm 1\}$ . However, there are constraints that the  $\mathcal{O}_I$  satisfy when the system is subject to periodic boundary conditions (compactified to a torus). One can show that

$$\prod_{I \in A} \mathcal{O}_I = \prod_{I \in B} \mathcal{O}_I = \mathbb{I}. \quad (3)$$

There are two constraints; therefore there are only  $2^{N-2}$  independent  $\{O_I = \pm 1\}$ . This implies, in particular, that there is a ground state degeneracy of  $2^2 = 4$ . (Notice that the ground state degeneracy is not associated with a symmetry. In particular, it is easy to show that  $\langle \sigma_I^{x,y,z} \rangle = 0$ .) This is a topological degeneracy and the eigenvalues of a set of two non-local (winding or topological) operators  $\mathcal{T}_{1,2}$  are needed to distinguish between the 4 degenerate ground states.

The operators  $\mathcal{T}_{1,2}$  can be constructed as follows. Let  $\mathcal{P}_l = \{I \mid i+j = l\}$  be a set of points along a horizontal line. Notice that sites on a line belong either all to sublattice  $A$  or all to sublattice  $B$ , for example  $\mathcal{P}_1 \subset A$  and  $\mathcal{P}_2 \subset B$ . Define

$$\mathcal{T}_1 = \prod_{I \in \mathcal{P}_1} \sigma_I^y \quad \mathcal{T}_2 = \prod_{I \in \mathcal{P}_2} \sigma_I^y. \quad (4)$$

It is simple to check that  $[\mathcal{T}_{1,2}, \mathcal{O}_I] = 0$  for all  $I$  and the two operators  $\mathcal{T}_{1,2}$  trivially commute. Hence the two eigenvalues  $\mathcal{T}_{1,2} = \pm 1$  of  $\mathcal{T}_{1,2}$  can distinguish the 4 degenerate ground states. This degeneracy has a topological origin and it scales with the genus of the surface.

The spectrum of the Hamiltonian Eq. (2) is that of a trivial set of  $N - 2$  free spins, determined by the list of eigenvalues  $\{O_I = \pm 1\}$  of all the  $\mathcal{O}_I$ , subject to the condition Eq. (3):  $E_{\{O_I\}} = -h \sum_I O_I$ . Excitations above the ground state ( $O_I = 1$  for all  $I$ ) are “defects” where  $O_I = -1$  in certain sites  $I$ . Because of the constraints in Eq. (3), the defects appear only in pairs. These defects have non-trivial quantum statistics: they are Abelian anyons with statistical angle different from that of fermions or bosons [7].

The equilibrium partition function (within a topological sector) is given by  $Z = \sum_{\{O_I = \pm 1\}} e^{\beta h \sum_I O_I}$ . In thermal equilibrium at temperature  $T$ , the thermal average  $\langle O_I \rangle = \tanh \frac{h}{T}$ , and the concentration or density of  $O_I = -1$  defects is  $c = \frac{1}{2} (1 - \tanh \frac{h}{T})$ . Notice that we have encountered a situation analogous to clas-

sical spin facilitated models [9], in particular the plaquette models displaying glassy dynamics [14, 16–18]: the thermodynamics is trivial in terms of non-interacting defect variables.

What about the dynamics of our quantum model? Although the spectrum of the model we are discussing is the same as that of free spins in a uniform magnetic field  $h$ , the variables  $O_I$  for different diamonds  $I$  *cannot* be independently changed. In fact, the operators  $\mathcal{O}_I$  involve four spins, shared by neighboring operators  $\mathcal{O}_{I'}$ . Under the action of any *local* spin operator, one cannot change the eigenvalue of  $O_I$  without changing the eigenvalues  $O_{I'}$  of its neighbors. What are the allowed, *physical* dynamical evolution rules for this quantum system? Can these dynamical rules lead to equilibration?

In order to endow the system with some physical dynamics, we couple the original physical spins to *individual* baths at temperature  $T$ . Here we do not consider “Turkish” baths of multiple spins; nonetheless, as long as the groups of spins sharing a bath are locally delimited in space, the results obtained below should remain qualitatively unchanged. Moreover, allowing the bath to communicate information through long-ranged couplings (via phonons, for instance) will not change the results, as long as it operates on delimited regions of space.

When the original individual spins are coupled to their baths, “flips” of the states of multiple  $\mathcal{O}_I$  sharing a given spin take place. Therefore, our model has a trivial spectrum but a highly correlated dynamics. It is this correlated dynamics that gives rise to non-trivial non-equilibrium behaviour.

We introduce the bath degrees of freedom as in the Feynman-Vernon influence functional approach [19] or Caldeira-Leggett dissipative quantum mechanics formulation [20, 21], by letting the Hamiltonian of the system plus bath be  $\hat{\mathcal{H}} = \hat{H} + \hat{H}_{\text{bath}} + \hat{H}_{\text{spin+bath}}$ , where  $\hat{H}$  is defined in Eq. (2), and

$$\hat{H}_{\text{bath}} = \sum_{I,\alpha} \int_0^\infty dx [\Pi_I^\alpha(t, x)]^2 + [\partial_x \Phi_I^\alpha(t, x)]^2 \quad (5a)$$

$$\hat{H}_{\text{spin/bath}} = \sum_{I,\alpha} g_\alpha \sigma_I^\alpha \Pi_I^\alpha(t, 0). \quad (5b)$$

The three components ( $\alpha = 1, 2, 3$ ) of the conjugate vector fields  $\Phi_I$  and  $\Pi_I$  obey the equal-time commutation relation  $[\Phi_I^\alpha(t, x), \Pi_J^{\alpha'}(t, x')] = i \delta_{IJ} \delta_{\alpha\alpha'} \delta(x - x')$ .

Notice that, for each site  $I$ , the bath-spin system can be viewed as an extended bosonic string that couples to a spin at the boundary  $x = 0$ . The coupling amplitudes are  $g_\alpha$ . One can in general choose anisotropic couplings, but the most general bath should contain all of  $g_{1,2,3}$ . In the quantum model, acting on a site  $I' \in P_I$  with one of  $\sigma_{I'}^x, \sigma_{I'}^y$ , or  $\sigma_{I'}^z$ , flips or not the eigenvalue  $O_I$  depending on whether  $\sigma_{I'}^{x,y,z} \mathcal{O}_I = \mp \mathcal{O}_I \sigma_{I'}^{x,y,z}$ , respectively.

If integrated out, the bath degrees of freedom away from the boundary  $x = 0$  lead to a non-local in time action and to dissipation effects. Instead of working with the dissipative action, let us follow the time evolution of the system plus bath and look at the possible evolution pathways of the quantum mechanical amplitudes of the system plus bath degrees of freedom. After evolution by time  $t$  from some initial state, the system is in a quantum mechanical superposition

$$|\Psi\rangle = \sum_{\{O_I=\pm 1\}} \Gamma_{\{O_I\}} |\{O_I\}\rangle \otimes |\Upsilon_{\{O_I\}}\rangle, \quad (6)$$

where  $|\Upsilon_{\{O_I\}}\rangle$  is a state in the bath Hilbert space with norm one. (Here we focus

on states in a single topological sector, although mixing sectors can be done by including the eigenvalues of the topological operators  $\mathcal{T}$ ; mixing is exponentially suppressed as the system size increases). The fact that the bath degrees of freedom couple to single quantum spins  $\sigma_I$  enters in the problem through the permitted channels for transferring amplitudes among the  $\Gamma_{\{O_I\}}$ .

The processes that transfer amplitude among the  $\Gamma_{\{O_I\}}$  correspond to different orders in perturbation theory on the system-bath coupling  $g_\alpha$ . There is also a thermal probability factor coming from the bath and that depends on the difference between the initial and final energy  $E_{\{O_I\}} = -h \sum_I O_I$  of the system. One class of paths is a *sequential* passage over states connected through order  $g_\alpha$  processes; this is a “semi-classical” type trajectory.

Within this restricted class of processes, we can make a connection to the classical plaquette models, particularly the 4-spin square plaquette model whose glassy properties have been studied in Refs. [18, 22, 23]. This classical model is obtained by defining diamond variables  $\tau_I$  in place of the  $\mathcal{O}_I$  as in Eq. (1) using *only*, say, the z-component  $\sigma^z$  for *all* four sites of the diamonds. Flipping an individual spin changes signs to all four  $\tau_I$  variables surrounding the spin. This multi-defect type dynamics makes it difficult for the system to relax to equilibrium. For example, if the temperature is lowered, in order to decrease the defect density, either four defects come together and annihilate ( $4 \rightarrow 0$  decay), or three defects become one ( $3 \rightarrow 1$  decay). However, the defects are not free to diffuse and come together. In order to move an isolated defect, it must first decay into three defects ( $1 \rightarrow 3$  production), then a pair can diffuse freely, and recombine with another defect elsewhere through a  $3 \rightarrow 1$  decay process. The final result is that the original defect (as well as the other defect elsewhere) moves by one lattice spacing and the total number of defects does not change (it first increases by 2 and then decreases by 2). Because of the initial  $1 \rightarrow 3$  production process, there is an energy barrier of  $2h$  to overcome. This activation barrier leads to recombination/equilibration times

$$t_{\text{seq.}} \sim \exp(2h/T) \quad (7)$$

that grow as temperature is lowered in an Arrhenius fashion [18].

In our model, the same situation is recovered if the coupling to the bath involves *only*  $\sigma^z$  components of the spins (i.e.,  $g_1 = g_2 = 0$ ). The Hamiltonian encompasses only  $\sigma^x$  and  $\sigma^y$  components and the action of a  $\sigma^z$  operator on a spin changes the eigenvalues of all four surrounding  $\mathcal{O}_I$ . One may then wonder how quantum tunnelling processes modify the behaviour of the system as compared to its classical counterpart. Recall that defect annihilation occurs only through virtual processes in which the number of defects is strictly larger in the intermediate (virtual) steps. At temperature  $T$ , the typical defect separation is  $\xi = c^{-1/2} \sim e^{h/2T}$ . Bringing them together requires tunnelling processes at least of order  $\xi$  in perturbation theory, which have an amplitude of order  $(g/h)^\xi$  (notice the energy denominator  $h$ ). This amplitude leads to recombination/equilibration times

$$t_{\text{tun.}} \sim \exp \left[ \ln(h/g) e^{h/2T} \right], \quad (8)$$

which grow extremely fast as the temperature is lowered. What we learn from this simple estimation is that quantum tunneling is less effective than classical sequential processes in thermalizing the system. This is counterintuitive to the notion that at low temperatures quantum tunneling under energy barriers remains an open process while classical mechanisms are suppressed due to thermal activation costs. The reason for this particular quantum freezing is simple: equilibration pro-



ceeds through activated defect recombination; as the density of defects decreases at low temperatures, the barrier *widths* increase and debilitate quantum tunneling. In passing, we note that in a finite system of size  $L$ , one must replace  $\xi$  by  $L$  in the estimation of the recombination/equilibration times,  $t_{\text{tun.}} \sim \exp[\ln(h/g) L]$ ; this time scale is also of the order of that for tunneling between two topological ground states in a finite system of size  $L$  [7].

Let us return to the issue of which component of spin enters in the coupling to the bath. The minimal bath coupling involves the z-component of the spin operator, for this component does not commute with *any* of the  $\mathcal{O}_I$  that contain that given spin. However, there is no *a priori* reason why the coupling should be restricted to z-components only. If the bath couples to x- and y-components as well, defects can diffuse freely without barriers (via  $1 \rightarrow 1$  processes), eliminating the need for  $1 \rightarrow 3$  defect production processes in order to bring them together and annihilate them. Simple defect diffusion leads to a diffusive equilibration time  $t_{\text{eq}} \sim L^2$  for a system of size  $L$  (polynomial in  $L$  with constant exponent).

Such dependence on the details of the bath coupling is removed in the 3D models we discuss next, one of which has even slower equilibration, as in fragile glasses.

### 3.2. 3D quantum strong glass

In the previous example, particle diffusion finds its origin in the fact that the x- or z-components of a spin commute with 2 out of the 4 surrounding diamonds. Therefore, defects can be created in pairs, not quadruplets, and single defect diffusion can take place through annihilation of a defect and creation of a neighbouring one via pair flip. In the example that follows (see also Refs. [8, 24]), six defect cells share each single spin, in such a way that acting with any component of the spin operators flips 4 cells and defect diffusion cannot occur.

The model displaying strong like glassiness is constructed on a three-dimensional (3D) face-centered cubic (fcc) Bravais lattice, spanned by the primitive vectors  $\mathbf{a}_1 = (1, 1, 0)/\sqrt{2}$ ,  $\mathbf{a}_2 = (0, 1, 1)/\sqrt{2}$ , and  $\mathbf{a}_3 = (1, 0, 1)/\sqrt{2}$ . Each site can be indexed by  $i, j, k \in \mathbb{Z}$ , and to shorten the notation, define a superindex  $I \equiv (i, j, k)$ . At every lattice site  $I$  one defines quantum spin  $S = 1/2$  operators  $\sigma_I^x$ ,  $\sigma_I^y$ , and  $\sigma_I^z$ .

The fcc lattice hosts sets of *octahedra*: the simplest one to visualize is the one assembled from the centers of the six faces of a cubic cell, as shown in Fig. 2. In addition to this simple set, there are three more sets of octahedra that can be assembled from sites both on faces and on corners of the cubic cells, totalling 4 such sets, which we label  $A, B, C$  and  $D$ .

It is simple to see that the total number of octahedra equals the number of spins: each lattice site  $I$  is the topmost vertex of a single octahedron. Define then  $P_I$  as the set of six lattice points in the octahedron with site  $I$  at its top. The six vertices are indexed by  $J_n(I)$ , for  $n = 1, \dots, 6$ , with one of the vertices  $J_1(I) = I$ . The six labels are assigned in such a way that the pairs  $\{J_1, J_4\}$ ,  $\{J_2, J_5\}$ ,  $\{J_3, J_6\}$  are diagonally opposite sites from one another. This number labeling is illustrated for a single octahedron in Fig. 2. From the one-to-one relation between a site  $I$  and the octahedra  $P_I$ , we can also partition the lattice sites into the four sets  $A, B, C$  and  $D$  of octahedra.

Now define the operators  $\mathcal{O}_I$  as

$$\mathcal{O}_I = \sigma_{J_1(I)}^z \sigma_{J_2(I)}^x \sigma_{J_3(I)}^y \sigma_{J_4(I)}^z \sigma_{J_5(I)}^x \sigma_{J_6(I)}^y. \quad (9)$$

These operators commute  $[\mathcal{O}_I, \mathcal{O}_{I'}] = 0$  for all pairs  $I, I'$ . Indeed, two distinct octahedra  $P_I$  and  $P_{I'}$  can either share 0, 1, or, 2 spins. If they share 0 spins, they

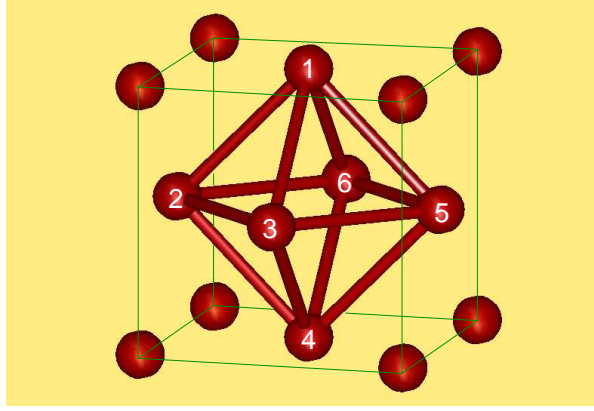


Figure 2. Cubic cell of an fcc lattice. The centers of the six faces form an octahedron, with its sites labeled from 1 (topmost) to 6. In addition to the set of octahedra formed by the face centered sites, there are three more sets of octahedra that can be assembled from sites both on faces and on corners of the cubic cells, totalling 4 such sets. Six-spin operators are defined on these octahedra using the  $\sigma^{x,y,z}$  components of spin on each vertex as described in the text.

trivially commute. If they share 1 spin, the component (x,y or z) of  $\sigma$  for that shared spin coincides for both  $\mathcal{O}_I$  and  $\mathcal{O}_{I'}$  (the two octahedra touch along one of their diagonals). If they share 2 spins, the components  $\sigma$  used in the definition of  $\mathcal{O}_I$  and  $\mathcal{O}_{I'}$  are different for both spins. Thus, there is a minus sign from commuting the spin operators from each of the shared spins, and the two minus signs cancel.

Consider the system Hamiltonian as in Eq. (2), which is trivially written in terms of the  $\mathcal{O}_I$  operators, but complicated in terms of the original spins  $\sigma_I$ . Because the  $\mathcal{O}_I$  commute, the eigenvalues of the Hamiltonian can be labeled by the list of eigenvalues  $\{O_I\}$  of all the  $\mathcal{O}_I$ . Notice that  $\mathcal{O}_I^2 = \mathbb{I}$  and so each  $O_I = \pm 1$ . In particular, the ground state corresponds to  $O_I = 1$  for all  $I$ .

Because the number of spins equals the number  $N$  of sites, one may naively expect that the list  $\{O_I = \pm 1\}$  exhausts the  $2^N$  states in the Hilbert space. However, there are constraints that the  $\mathcal{O}_I$  satisfy when the system is subject to periodic boundary conditions (compactified). One can show that

$$\prod_{I \in A} \mathcal{O}_I = \prod_{I \in B} \mathcal{O}_I = \prod_{I \in C} \mathcal{O}_I = \prod_{I \in D} \mathcal{O}_I = \mathbb{I}. \quad (10)$$

There are four constraints; therefore there are only  $2^{N-4}$  independent  $\{O_I = \pm 1\}$  and there is a ground state degeneracy of  $2^4 = 16$  (for a thorough discussion of this degeneracy and its dependence on boundary conditions, see Ref. [24]). This is a topological degeneracy and the number of ground states scales with the genus of the manifold the system is defined on. The eigenvalues of a set of four non-local (topological) operators  $\mathcal{T}_{1,2,3,4}$  are needed to distinguish between the 16 degenerate ground states.

The operators  $\mathcal{T}_{1,2,3,4}$  can be constructed as follows. Let  $\mathcal{P}_l = \{I \mid j+k=l\}$  be a set of points along a horizontal plane. Notice that each plane contains sites in only two of the four sublattices  $A, B, C, D$ . For example  $\mathcal{P}_1 \subset A \cup B$  and  $\mathcal{P}_2 \subset C \cup D$ . Define

$$\mathcal{T}_1 = \prod_{I \in \mathcal{P}_1 \cap A} \sigma_I^z \quad \mathcal{T}_2 = \prod_{I \in \mathcal{P}_1 \cap B} \sigma_I^z \quad \mathcal{T}_3 = \prod_{I \in \mathcal{P}_2 \cap C} \sigma_I^z \quad \mathcal{T}_4 = \prod_{I \in \mathcal{P}_2 \cap D} \sigma_I^z. \quad (11)$$

It is simple to check that  $[\mathcal{T}_{1,2,3,4}, \mathcal{O}_I] = 0$  for all  $I$ , and the  $\mathcal{T}_{1,2,3,4}$  trivially commute among themselves. Hence the four eigenvalues  $T_{1,2,3,4} = \pm 1$  of  $\mathcal{T}_{1,2,3,4}$  can

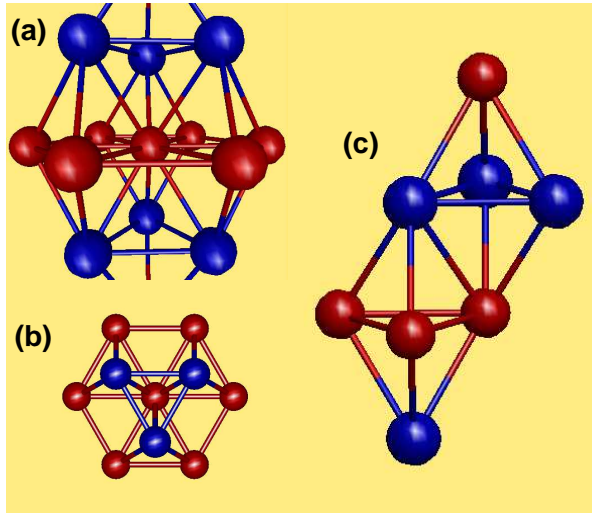


Figure 3. Sites of an hcp (hexagonal close-packed) lattice. (a) The hcp lattice is comprised of two interpenetrating hexagonal lattices, which can be alternatively seen as stacked triangular lattices, shown in red and blue. Prisms are defined as sets of five sites, two of which belong to one sublattice (top and bottom of the prism), and three of which belong to the other and form a triangle that lies in the layer in between the top and bottom sites of the prism. Five-spin interactions are defined on each prism as explained in the text. (b) Top view of the hcp lattice, which shows that the blue sites stack on top of the red upward pointing triangles, and the red sites stack on top of the downward pointing blue triangles. (c) Two prisms with topmost sites belonging to different sublattices can share a common edge and the five-spin operators defined on the two prisms commute because minus signs from commuting the  $\sigma^x$  and  $\sigma^z$  components appear twice, once for each shared site, and cancel.

distinguish the 16 degenerate ground states.

In this model one can verify that, whichever component of spin enters in the coupling to the bath, it is impossible to flip only a pair of defects and thus there is no mechanism for defect diffusion. The reason is that any site is shared by 6 octahedra, and the operators  $\mathcal{O}_I$  for these cells are such that one can divide the 6 into 3 groups of 2 octahedra that will have in their definitions, respectively, the x, y, and z component of spin operators at the shared site. Acting with either of the three components of the spin operator on this shared site will flip at least four defects.

Quantum glassiness, i.e., the behaviour in Eq. (8) leading to  $\tau_q \sim \exp(L)$ , is thus protected against any local bath. On the other hand, as soon as we leave the  $T = 0$  limit, the system size dependence of the relaxation time scales changes radically. Indeed, the energy barrier to defect diffusion is only a ‘one-step’ process. As soon as  $1 \rightarrow 3$  decays are allowed to take place thermally, any two of the three new defects can diffuse freely across the system. The time scales for diffusion are simply rescaled by the factor  $t_{\text{seq.}} \sim \exp(2h/T)$ , Eq. (7), but the system size dependence remain only  $\tau_c \sim \text{poly}(L)$ .

### 3.3. 3D quantum fragile glass

The model displaying fragile-like glassiness is constructed on a three-dimensional (3D) hexagonal close-packed lattice, shown in Fig. 3. The lattice can be viewed as two interpenetrating simple hexagonal Bravais lattices displaced from one another by  $\mathbf{a}_1/3 + \mathbf{a}_2/3 + \mathbf{a}_3/2$ , where  $\mathbf{a}_1 = (1, 0, 0)$ ,  $\mathbf{a}_2 = (1, \sqrt{3}, 0)/2$ , and  $\mathbf{a}_3 = (0, 0, 1)$  are the primitive vectors of the simple hexagonal lattice. The sites belonging to the two intercalating lattices are shown in red and blue color in Fig. 3. Each site can be labeled by  $i, j, k \in \mathbb{Z}$  that index a site in the Bravais lattice spanned by  $\mathbf{a}_{1,2,3}$ , plus  $q = 0, 1$  that indexes each of the two sublattices – to shorten the notation,

define a superindex  $I \equiv (i, j, k; q)$ . At every lattice site  $I$  one defines quantum spin  $S = 1/2$  operators  $\sigma_I^x$ ,  $\sigma_I^y$ , and  $\sigma_I^z$ .

Define now a *prism* cell  $P_I$  that contains five lattice sites  $J_n(I)$ , for  $n = 1, \dots, 5$  as follows. For a given lattice site  $I$ , the prism  $P_I$  contains the site  $J_1(I) = I$ , which belongs to one sublattice of the hexagonal close-packed lattice, the three sites that belong to the other sublattice and that form an elementary triangle (sites  $J_2, J_3, J_4$ ) just below the site  $I$ , and finally the site  $J_5(I)$  just below that triangle, which belongs to the same sublattice as site  $I$ . [In terms of the lattice indices,  $J_5(I) \equiv (i, j, k-1; q)$  if  $I \equiv (i, j, k; q)$ .] An example of two prisms is shown in Fig. 3c. Notice that the two prisms shown share a common edge, and that their tops belong to distinct (red and blue) sublattices. The total number of prisms equals the number of spins: each lattice site  $I$  is the top vertex of a single prism.

Now define the operators  $\mathcal{O}_I$  as

$$\mathcal{O}_I = \sigma_{J_1(I)}^z \sigma_{J_2(I)}^x \sigma_{J_3(I)}^x \sigma_{J_4(I)}^x \sigma_{J_5(I)}^z. \quad (12)$$

The operators commute,  $[\mathcal{O}_I, \mathcal{O}_{I'}] = 0$ , for all pairs  $I, I'$ . Indeed, if  $I, I'$  belong to the same sublattice and the prisms  $P_I, P_{I'}$  share a vertex, then they trivially commute as they both involve the same component (x or z) of the spin operators  $\sigma$  at the shared site. If they belong to distinct sublattices, they either share 0 spins or an edge with 2 spins, as shown in Fig. 3. If they share 2 spins, the minus signs from commuting the x and z components of spin in each of the shared sites appear an even number of times.

Consider the system Hamiltonian as in Eq. (2), which is trivially written in terms of the  $\mathcal{O}_I$  operators, but complicated in terms of the original spins  $\sigma_I$ . Because the  $\mathcal{O}_I$  commute, the eigenvalues of the Hamiltonian can be labeled by the list of eigenvalues  $\{O_I\}$  of all the  $\mathcal{O}_I$ . Notice that  $\mathcal{O}_I^2 = \mathbb{I}$ , and so each  $O_I = \pm 1$ . In particular, the ground state corresponds to  $O_I = 1$  for all  $I$ .

Because the number of spins equals the number  $N$  of sites, one may naively expect that the list  $\{O_I = \pm 1\}$  exhausts the  $2^N$  states in the Hilbert space. However, there are constraints that the  $\mathcal{O}_I$  satisfy when the system is subject to periodic boundary conditions (compactified). Each of the two sublattices ( $q = 0, 1$ ) of the hexagonal close-packed structure can be further subdivided into  $A_q, B_q$  or  $C_q$  according to the three sublattices of the tripartite triangular stacks of the simple hexagonal lattice. (All in all, there are six sublattices  $A_{0,1}, B_{0,1}$  and  $C_{0,1}$ .) One can show that

$$\prod_{I \in A_q \cup B_q} \mathcal{O}_I = \prod_{I \in B_q \cup C_q} \mathcal{O}_I = \prod_{I \in C_q \cup A_q} \mathcal{O}_I = \mathbb{I}. \quad (13)$$

These are six constraints, but only four are independent, because the product of the three products in Eq. (13) for the same  $q$  is trivially the identity. Therefore there are only  $2^{N-4}$  independent  $\{O_I = \pm 1\}$ . This implies, in particular, that there is a ground state degeneracy of  $2^4 = 16$  which is topological in nature and the number of ground states scales with the genus of the manifold the system is defined on. The eigenvalues of a set of four non-local (topological) operators  $\mathcal{T}_{1,2,3,4}$  are needed to distinguish between the 16 degenerate ground states.

The operators  $\mathcal{T}_{1,2,3,4}$  can be constructed as follows. Let the plane  $\mathcal{P}_{k,q}$  be the

set containing sites with fixed  $k$  and  $q$ . Let

$$\mathcal{T}_1 = \prod_{I \in \mathcal{P}_{1,0} \cap (A_0 \cup B_0)} \sigma_I^z \quad \mathcal{T}_2 = \prod_{I \in \mathcal{P}_{1,0} \cap (B_0 \cup C_0)} \sigma_I^z \quad (14a)$$

$$\mathcal{T}_3 = \prod_{I \in \mathcal{P}_{1,1} \cap (A_1 \cup B_1)} \sigma_I^z \quad \mathcal{T}_4 = \prod_{I \in \mathcal{P}_{1,1} \cap (B_1 \cup C_1)} \sigma_I^z. \quad (14b)$$

It is simple to check that  $[\mathcal{T}_{1,2,3,4}, \mathcal{O}_I] = 0$  for all  $I$ , and the  $\mathcal{T}_{1,2,3,4}$  trivially commute among themselves. Hence the four eigenvalues  $T_{1,2,3,4} = \pm 1$  of  $\mathcal{T}_{1,2,3,4}$  can distinguish the 16 degenerate ground states.

There are relations between this 3D model and a 2D classical triangular plaquette model which has glassy behavior [14, 16, 17]. The 2D triangular plaquette model has Ising spin variables defined on the sites of a triangular lattice and a 3-spin interaction which is the product of the Ising variables on the downward pointing triangular plaquettes only. Plaquette Ising variables (the 3-spin products) are defined at the centre of the downward triangles, which behave thermodynamically as free Ising spins in a magnetic field. However, the dynamics is rather non-trivial in terms of the plaquette variables, for flipping an original spin corresponds to flipping all three surrounding plaquettes.

In our 3D model, each quantum spin  $\sigma_I$  is shared by 5 prisms: 3 whose centers are on the same plane, and 2 whose centers are immediately above and below site  $I$ . If the system-bath coupling contains the  $\sigma^y$  spin component, all 5 prisms are flipped. The  $\sigma^z$  and  $\sigma^x$  components flip either the eigenvalues of the 3 prisms on the plane or the 2 prisms on the vertical direction, respectively. Flipping the eigenvalues of 2 prisms in the vertical direction leads to defect diffusion, but only in that direction.

To connect our 3D quantum model to the triangular plaquette model, consider a compactified slab (periodic boundary conditions) in the third dimension (parallel to  $\mathbf{a}_3$ ), with  $M$  layers. Because of the periodic boundary conditions, the odd-even parity of the defect number is conserved along vertically stacked prisms regardless of the system-bath spin-flip operator,  $\sigma^x$ ,  $\sigma^y$ , or  $\sigma^z$ . The defect number parity can be captured by defining the following operator (recall  $I \equiv (i, j, k; q)$ ):

$$\tau_{i,j;q} = \prod_k \mathcal{O}_{(i,j,k;q)}. \quad (15)$$

It is also useful to define a similar product over the third dimension for the original spins:

$$s_{i,j;q} = \prod_k \sigma_{(i,j,k;q)}^x. \quad (16)$$

These “slab” operators allows us to concentrate on subspaces of the Hilbert space with a given set of  $\tau_{i,j;q}$  instead of the states with given  $\mathcal{O}_{i,j,k;q}$ . There are dynamical processes that transfer quantum mechanical amplitudes within and between these subspaces labeled by  $\tau_{i,j;q}$ ; we can argue that the system is glassy by simply looking at the processes that transfer amplitude between the subspaces.

The variables  $\tau_{i,j;q}$  and  $s_{i,j;q}$  can effectively be used to relate our quantum model to two 2D systems ( $q = 0$  or red, and  $q = 1$  or blue) defined on sites labeled by  $(i, j; q)$  of two distinct triangular lattices. The variables  $s_{i,j;q}$  can be related to the original spin variables in the models of Refs. [14, 16, 17]. In particular, one can

relate the  $s_{i,j;q}$  and the  $\tau_{i,j;q}$  using Newton's binomial coefficients through

$$s_{i,j;q} = \prod_{mn} [\tau_{n,m;q}]^{\binom{j-n}{i-m}}. \quad (17)$$

Using the Pascal triangle relation  $\binom{j+1-n}{i+1-m} = \binom{j-n}{i-m} + \binom{j-n}{i+1-m}$  one can show that indeed the defect variables correspond to

$$\tau_{i,j;q} = s_{i,j;q} s_{i+1,j;q} s_{i,j+1;q}. \quad (18)$$

We can focus again on two classes of processes: sequential passage over states connected through order  $g_\alpha$  processes ("semi-classical" type trajectories), and quantum tunneling process. The analysis of the sequential processes is similar to that of the classical 2D models [14, 16, 17] and goes as follows. Single flips of  $s$  correspond to concomitant flips of three  $\tau$  defects. Defects can only be annihilated in triplets. The defects are not free to diffuse and come together; instead, they move through the production of more defects. For example, a defect can decay into two more defects, by flipping one  $s$  variable. Now, in order to bring three defects separated by a distance  $\xi$  together, one has to go through intermediate steps with a large number of defects that are created. There is a hierarchical organization of these intermediate processes; equilateral triangles of size  $\xi = 2^\ell$  require the creation of  $\ell$  extra intermediate defects. Hence there is an energy barrier of order  $\ell h$  to be overcome. For a typical equilibrium separation  $\xi = c^{-1/2} \sim e^{h/2T}$ , the barriers to be overcome in the equilibration processes are of order  $h^2/(T 2 \ln 2)$ . Hence, the equilibration time scales as

$$t_{\text{seq.}} \sim \exp \left[ \frac{(h/T)^2}{2 \ln 2} \right], \quad (19)$$

a much slower relaxation than the Arrhenius one, Eq. (7), for the model discussed in Section 3.2.

Through quantum tunneling, defect annihilation can occur via virtual processes in which the number of defects is strictly larger in the intermediate (virtual) steps. The order in perturbation theory in  $g$  grows very fast with defect separation. An example is shown in Fig. 4; basically, to annihilate three defects at the corners of an equilateral triangle of size  $\xi = 2^\ell$ , one must flip  $3^\ell$  original spins laying on a mold defined by a Sierpinski gasket. (Notice that here the hierarchy is built starting from the microscopic scale.) In perturbation theory the quantum recombination process has an amplitude of order  $(g/h)^{3^\ell}$ , which leads to recombination/equilibration times

$$t_{\text{tun.}} \sim \exp \left[ \ln \left( \frac{h}{g} \right) \exp \left( \frac{\ln 3}{2 \ln 2} \frac{h}{T} \right) \right], \quad (20)$$

which grows extremely fast as the temperature is lowered. Again, we learn from this simple estimation that quantum tunneling is less effective than classical sequential processes in thermalizing the system.

In a finite size system, the limiting time scale will be set by  $\xi \sim L$ , whereby

$$\tau_q \sim \left( \frac{g}{h} \right)^{L^{\log_2(3)}} = \exp \left[ L^{\log_2(3)} \ln \left( \frac{g}{h} \right) \right] \quad (21)$$

leading to a quantum mechanical exponential dependence on system size in contrast with the polynomial scaling of the classical (activated) time scales that become

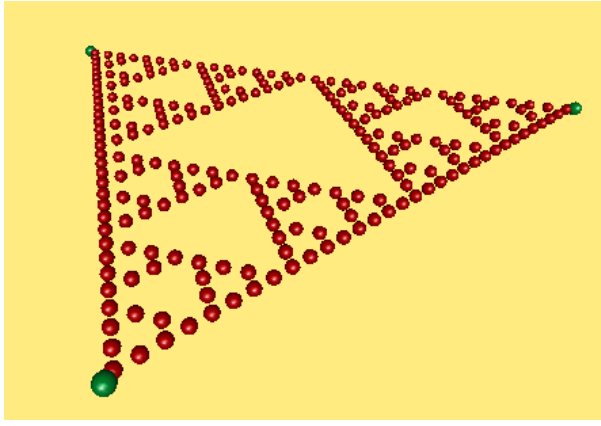


Figure 4. To annihilate three defects (shown in green) at the corners of an equilateral triangle, one must flip the spins in a “fractal” membrane (containing sites shown in red) that stretches between the defects. For a triangle of size  $2^\ell$ , there are  $3^\ell$  sites in the membrane. The annihilation of the three defects through quantum tunneling is a virtual process of order the number of sites that are involved (red sites). Hence, the amplitude for the quantum tunneling process vanishes exponentially with the “volume” of the membrane.

available at any finite temperature,

$$\tau_c \sim \exp \left[ \frac{h \log_2(L)}{T} \right] = L^{h/T \ln 2}, \quad (22)$$

as in the long time scale limit  $\xi \rightarrow L$ , the classical energy barriers  $\ell h$  tend to the value  $h \log_2(L)$ .

#### 4. Note on perturbative approaches

It is interesting to comment briefly on more generic approaches to study equilibration in quantum systems coupled to a bath, specifically in regards to quantum glasses with exponential time scales.

Quantum systems in contact with a reservoir are characterized by mixed ensembles of states that are best described using von Neumann’s density matrix formalism [25, 26]. At equilibrium, the density operator is given by  $\hat{\rho} = e^{-\beta \hat{H}}/Z$  in the canonical ensemble, where  $\hat{H}$  is the Hamiltonian of the system,  $\beta = 1/T$  is the inverse temperature of the reservoir (and of the system of interest, *at equilibrium*), and  $Z = \text{tr}(e^{-\beta \hat{H}})$  is the canonical partition function. The expectation value of any operator  $\hat{O}$  in this mixed ensemble is given by  $\text{tr}(\hat{\rho} \hat{O})$ . Therefore, the characterisation of the properties of a quantum system at equilibrium is essentially a spectral problem. Describing the low temperature properties of a system, for example, requires the understanding of the ground state, its symmetries (or lack thereof) and its quantum orders [27], and its low lying excitations. In particular, at zero temperature, the system goes to its ground state. In the case of a quantum many-body system, if parameters in the Hamiltonian  $\hat{H}$  are tuned, the ground state can change its symmetries or its quantum orders through quantum phase transitions.

The time evolution of a system  $s$  in contact with a reservoir  $b$  and total Hamiltonian

$$H = H_s + H_b + V \equiv H_0 + V \quad (23)$$

is described by the Liouville-von Neumann equation

$$\frac{d\rho(t)}{dt} = -i [H, \rho(t)], \quad (24)$$

where  $\rho(t) = \exp(iHt) \rho \exp(-iHt)$  is the time-dependent density matrix of the system plus bath, and we use the convention  $\hbar = 1$ . (Without loss of generality, we assume that  $H$  does not depend directly on time.) It is customary to recast Eq. (24) in the interaction picture format,

$$\rho_I(t) \equiv e^{-iH_0 t} e^{iHt} \rho e^{-iHt} e^{iH_0 t} \quad (25)$$

$$V_I(t) \equiv e^{-iH_0 t} V e^{iH_0 t} \quad (26)$$

whereby

$$\frac{d\rho_I(t)}{dt} = -i [V_I(t), \rho_I(t)]. \quad (27)$$

Note that  $\rho_I(0) = \rho(0) = \rho$ . If we are interested in the evolution of the system alone, we need to trace over the degrees of freedom of the reservoir,

$$\rho_I^{(s)}(t) \equiv \text{tr}_b[\rho_I(t)] \quad (28)$$

$$\frac{d\rho_I^{(s)}(t)}{dt} = -i \text{tr}_b [V_I(t), \rho_I(t)]. \quad (29)$$

The right hand side of Eq. (29) results in a linear super-operator acting on  $\rho_I^{(s)}(t)$ . By comparison with its classical counterpart, i.e., the transition matrix in a Master equation, the eigenvalues of the super-operator determine the equilibration rates of the quantum system coupled to the bath. Following Ref. [28], one could then symmetrise the super-operator and reinterpret it as a fictitious quantum ‘Hamiltonian’ acting on the space of density matrices  $\rho$ . The appearance of diverging time scales in the quantum system would then correspond to a quantum phase transition in the associated ‘Hamiltonian’. Note that at the quantum level, the correspondence between the original Hamiltonian and the fictitious one occurs interestingly in the same number of dimensions for both systems.

Unfortunately, taking the trace of the right hand side of Eq. (29) to find the super-operator acting on  $\rho_I^{(s)}(t)$  is in general a tall order. A common approach consists of expanding the commutator  $[V_I(t), \rho_I(t)]$  perturbatively in the interaction between system and reservoir, leading to the recursive equation

$$\begin{aligned} \frac{d\rho_I(t)}{dt} &= -i [V_I(t), \rho_I(0)] \\ &+ \sum_{n=1}^{\infty} (-i)^{n+1} \int_0^t d\tau_1 \int_0^{\tau_1} d\tau_2 \dots \int_0^{\tau_{n-1}} d\tau_n [V_I(t), [V_I(\tau_1), \dots [V_I(\tau_n), \rho_I(0)]] \dots] \\ &= -i [V_I(t), \rho_I(0)] - \int_0^t d\tau [V_I(t), [V_I(\tau), \rho_I(0)]] + \dots \end{aligned} \quad (30)$$

Carrying out the trace becomes now feasible under the conventional assumption that the initial density matrix factorises into system and bath,  $\rho_I(0) = \rho^{(s)} \otimes \rho^{(b)}$ . However, one needs to consider that each order in the expansion enables tunnelling



processes in the system-bath interaction  $V$  up to that very same order. As discussed in Sec. 2 and as seen in the concrete examples in Sec. 3, the relaxation processes typical of quantum glasses require tunnelling under barriers whose width scales with system size. Such processes would be all together forbidden at any finite order in the perturbative expansion. One could view this as a *signature of quantum glassiness*: the appearance of disconnected sectors in the quantum dynamics of the system at any finite order in perturbation theory.

## 5. Conclusions

There are plenty of systems in nature that recalcitrantly avoid equilibration with the environment. When their time scales become impractically large to measure, these systems are conventionally referred to as glasses.

In order to investigate how this phenomenon comes about, it is reasonable to distinguish between different classes of slow dynamics according to the way that their equilibration times scale with their physical size. One can draw a parallel with computational complexity. When the system does not manage to equilibrate in  $\text{poly}(L)$  time, it is because nature's algorithm for (local) dynamics is not efficient. Systems with  $\exp(L)$  time scales are computationally hard given nature's resources. [We note in passing that, just as in the case of the definition of computational complexity classes, one must allow for considerations of practical importance: time scales can diverge as a function of temperature while remaining polynomial in  $L$ .]

What happens when temperature is lowered all the way down to  $T = 0$ ? Because absolute zero temperature freezes out all classical activation processes, quantum tunneling is all that is left to dynamics. The relevant issue then becomes which kind of tunneling barriers remain to surpass so as to reach the ground state in the presence of a zero temperature bath. It is the nature of these barriers that separates systems with relaxation times that are exponential vs. polynomial in  $L$ , and therefore separates systems that are quantum glasses (hard, for nature's algorithm) from those that are not.

In this paper we discussed these issues and constructed explicit examples of systems with exponential time scales at zero temperature. These systems are devoid of disorder or local symmetry breaking, but rather exhibit a non-local form of order known as topological order. As such, they ought to be considered examples of topological quantum glasses. We showed how our *local* quantum Hamiltonians resist equilibration with a thermal bath and glassiness is "protected" against thermal equilibration with *any* bath, provided that it couples *locally* with the *physical* degrees of freedom of the system.

It is often believed that quantum tunneling provides an escape route against classical dynamical slowdown caused by thermal energy barriers as the temperature is lowered. In the systems presented here, classical sequential processes are more effective than quantum tunneling processes in the limit  $T \rightarrow 0$ . The reason for the freezing of quantum tunneling is that equilibration is through *activated* defect recombination; as the density of defects decreases at low temperatures, the barrier *widths* increase and eventually become as large as the size of the system.

We also discussed briefly generic approaches to study equilibration in quantum systems in contact with a reservoir, starting from the Liouville-von Neumann equation. Following this route one can in principle arrive at the quantum mechanical counterpart to the classical Master equation for the equilibration of probabilities. The role played by the transition matrix is here taken by a super-operator, whose spectrum controls the relaxation properties of the system. It is intriguing to speculate that a quantum-to-quantum mapping akin to the classical-to-quantum

correspondence discussed in Ref. [28] would lead to the formulation of a fictitious quantum mechanical system in the same number of dimension of the original one, where quantum dynamical transitions would appear as static, zero temperature quantum phase transitions. However, constructing the super-operator is in general a tall order and at best one can do so order by order in perturbation theory. One should note however that truncating the expansion to any fixed order in perturbation theory on the system/bath coupling disconnects the space of states. In order to study quantum glassy systems, it is necessary to go to all the way to order  $L$  in the perturbation expansion, accessing matrix elements that are exponentially small, and therefore time scales that are exponentially large in  $L$ .

### Acknowledgement(s)

This work was supported in part by EPSRC Postdoctoral Research Fellowship EP/G049394/1 (C.C.), and by DOE Grant DEFG02-06ER46316 (C.C.).

### References

- [1] C.A. Angell, Proc. Natl. Acad. Sci. 92 (1995) p.6675.
- [2] D. Sherrington and F. Kirkpatrick, Phys. Rev. Lett. 35 (1975) p.1792.
- [3] A. Crisanti and H.J. Sommers, Z. Phys. B 87 (1992) p.341.
- [4] A. Crisanti, H. Horner and H.J. Sommers, Z. Phys. B 92 (1993) p.257.
- [5] X.G. Wen, Int. J. Mod. Phys. B 4 (1990) p.239.
- [6] X.G. Wen, Adv. Phys. 44 (1995) p.405.
- [7] A.Y. Kitaev, Ann. of Phys. 303 (2003) p.2.
- [8] C. Chamon, Phys. Rev. Lett. 94 (2005) p.040402.
- [9] F. Ritort and P. Sollich, Adv. Phys. 52 (2003) p.219.
- [10] J.P. Garrahan and D. Chandler, Proc. Natl. Acad. Sci. 100 (2003) p.9710.
- [11] M.E.J. Newman and C. Moore, Phys. Rev. E 60 (1999) p.5068.
- [12] J.P. Garrahan and M.E.J. Newman, Phys. Rev. E 62 (2000) p.7670.
- [13] A. Buhot and J.P. Garrahan, Phys. Rev. Lett. 88 (2002) p.225702.
- [14] J.P. Garrahan, J. Phys. Cond. Matt. 14 (2002) p.1571.
- [15] X.G. Wen, Phys. Rev. Lett. 90 (2003) p.016803.
- [16] M.E.J. Newman and C. Moore, Phys. Rev. E 60 (1999) p.5068.
- [17] J.P. Garrahan and M.E.J. Newman, Phys. Rev. E 62 (2000) p.7670.
- [18] A. Buhot and J.P. Garrahan, Phys. Rev. Lett. 88 (2002) p.225702.
- [19] R.P. Feynman and F.L. Vernon Jr., Ann. of Phys. 24 (1963) p.118.
- [20] A.O. Caldeira and A.J. Leggett, Phys. Rev. Lett. 46 (1981) p.211.
- [21] A.O. Caldeira and A.J. Leggett, Ann. of Phys. 149 (1983) p.374.
- [22] D. Alvarez, S. Franz and F. Ritort, Phys. Rev. B 54 (1996) p.9756.
- [23] A. Lipowski, J. Phys. A 30 (1997) p.7365.
- [24] S. Bravyi, B. Leemhuis and B.M. Terhal, Ann. of Phys. 326 (2011) p.839.
- [25] J. Neumann von, Göttinger Nachrichten (1927) p.245.
- [26] K. Blum *Density matrix theory and applications*, Plenum Press, 1996.
- [27] X.G. Wen, Phys. Rev. B 65 (2002) p.165113.
- [28] C. Castelnuovo, C. Chamon and D. Sherrington, Phys. Rev. B 81 (2010) p.184303.